
Project # 35: Characterization of Microstructures and Mechanical Properties in Linear Friction Welding and Electron Beam Additive Manufacturing Ti-6Al-4V

***Fall 2019 Semi-Annual Meeting
Colorado School of Mines, Golden, CO
October 9 - 11, 2019***

Student: Michael Mendoza (ISU)

Faculty: Peter Collins ISU

Industrial Mentors: Honeywell



**Center Proprietary – Terms of CANFSA
Membership Agreement Apply**

Project 35: Characterization of Microstructures and Mechanical Properties in Linear Friction Welding and Electron Beam Additive Manufacturing Ti-6Al-4V



- Student: Michael Mendoza (ISU)
- Advisor(s): Peter Collins (ISU)

Project Duration
PhD: January 2017 to December 2019

- **Problem:** Linear Friction Welding (LFW) offers cost reduction for aircraft structural components production. However, the information about its microstructure and mechanical properties is still limited.
- **Objective:** Characterize local microstructures (LFW) and their relationship with mechanical properties
- **Benefit:** The understanding of microstructure-properties relationship of LFW will improve manufacturing efficiency of aircraft components.

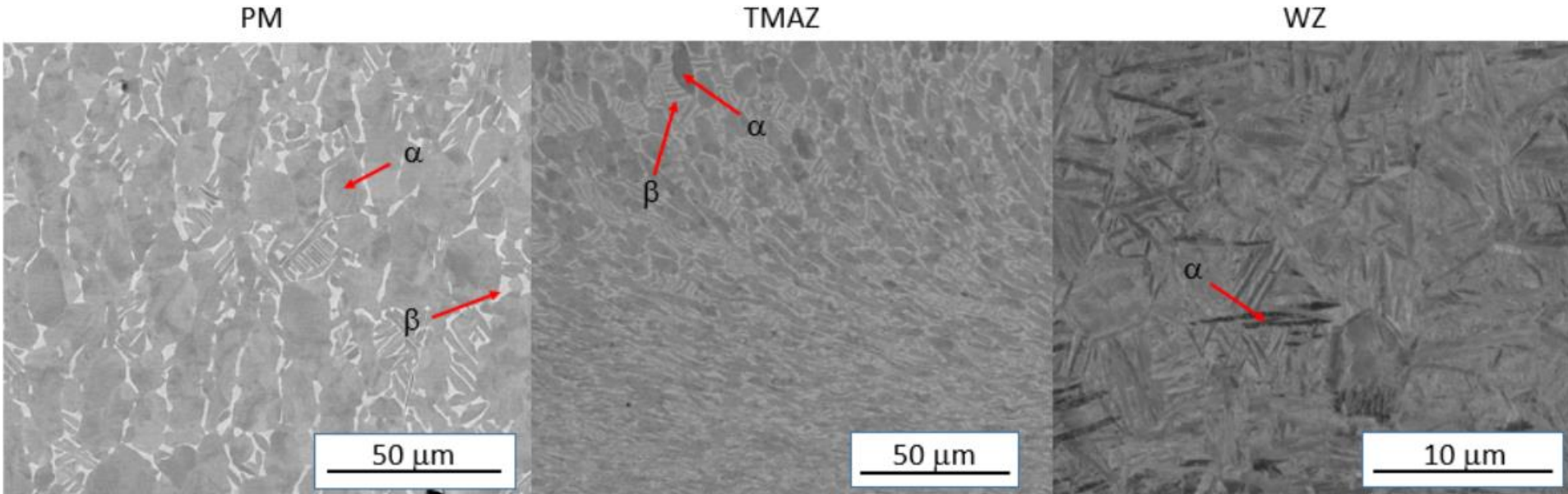
Recent Progress

- TEM-PED data with dislocation density calculation on all three LFW zones.
- Conventional four-point bending fatigue data and analysis of results.

Metrics

Description	% Complete	Status
1. Literature review	95%	●
2. Microstructure and tensile properties of dogbone samples within the individual three LFW zones	100%	●
3. Conventional fatigue analysis (four-point bending test) of local microstructures EBAM-Ti-6Al-4V	100%	●
4. Simulation and design (Comsol) of ultrasonic fatigue on local microstructures of EBAM-Ti-6Al-4V	100%	●
5. Ultrasonic fatigue test design and modifications	85%	●

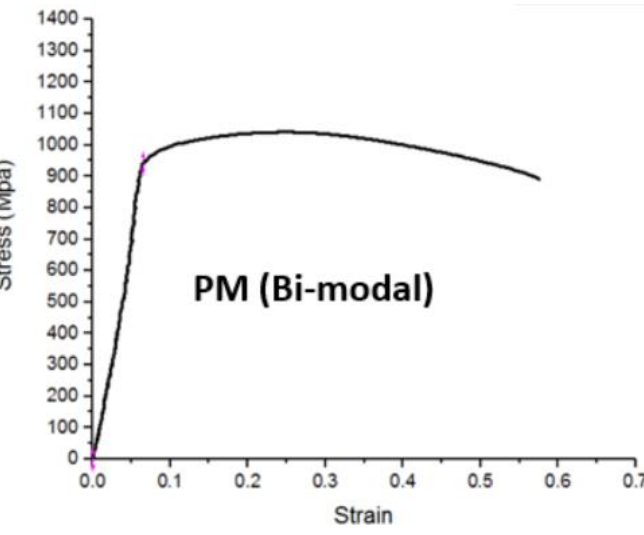
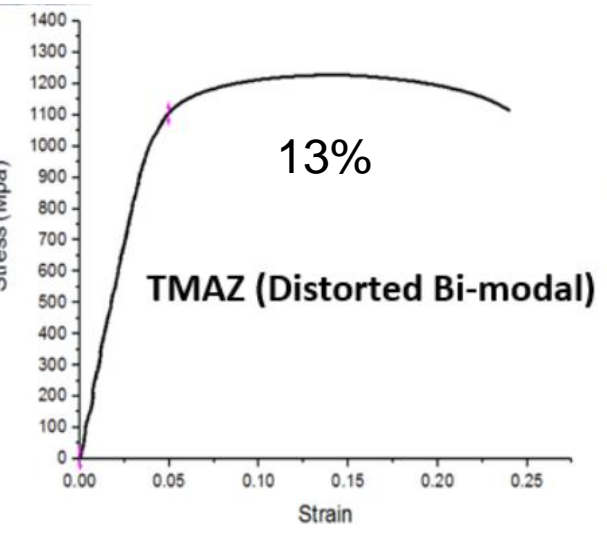
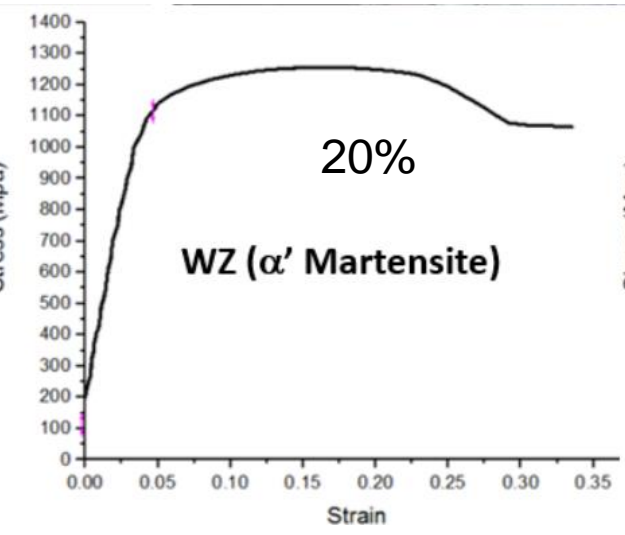
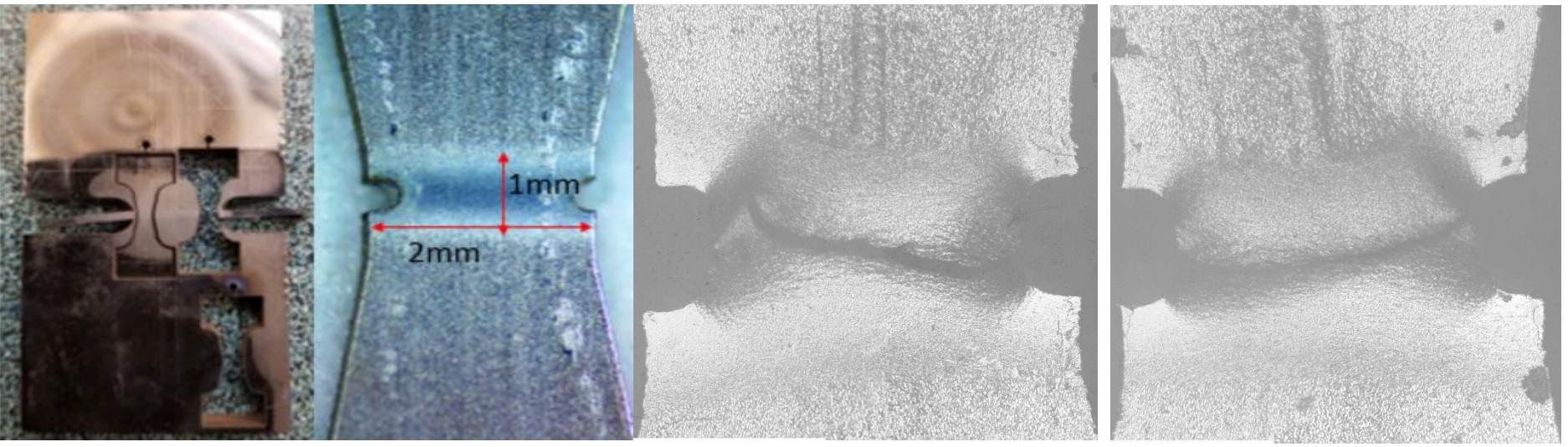
Linear Friction Welding (LFW) Zones



Backscatter electron micrographs on each zone

- PM - parent material with a bi-modal microstructure (i.e. primary α_p grains surrounded by α lamellar microstructure of α laths in a β matrix).
- TMAZ - Thermomechanical affected zone with a distorted bi-modal microstructure.
- WZ - Welded zone with a refined martensitic α' (needle like) laths in a β matrix.

Tensile Properties of LFW-Ti-6Al-4V



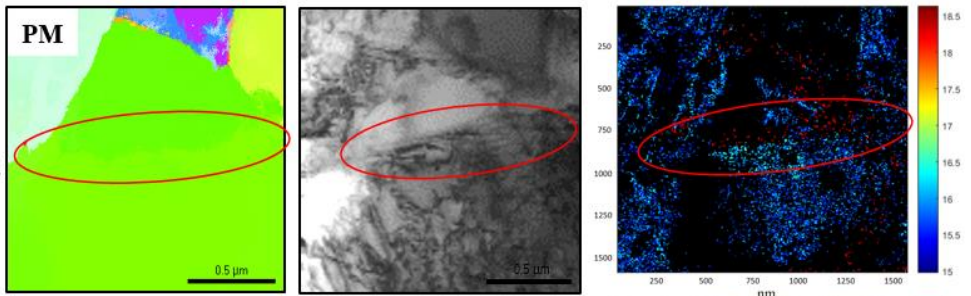
Dislocation Density Analysis of LFW Zones



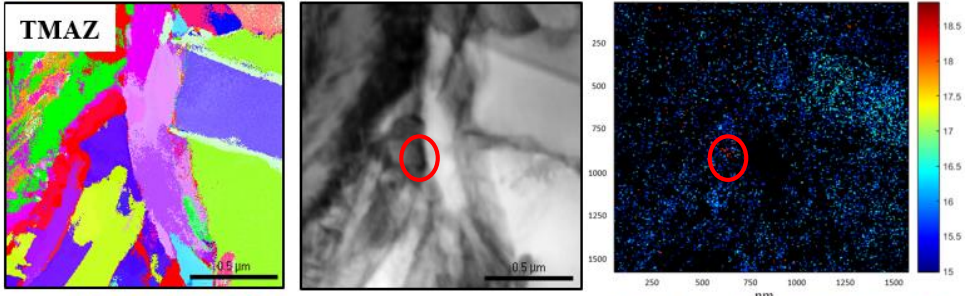
The dislocation density calculation from PED results indicate an unexpected higher average value for the parent material (PM) compared with the TMAZ and WZ. However, some considerations have to be analyzed:

1. The parent material does not undergo plastic deformation during LFW process
2. Bending contours created during foil preparation can artificially increase the local misorientation which in turn increases the dislocation density calculation.
3. The indexing process can mistakenly identify grain boundaries or smaller grains (islands) within larger grains due to a known 180-degree ambiguity

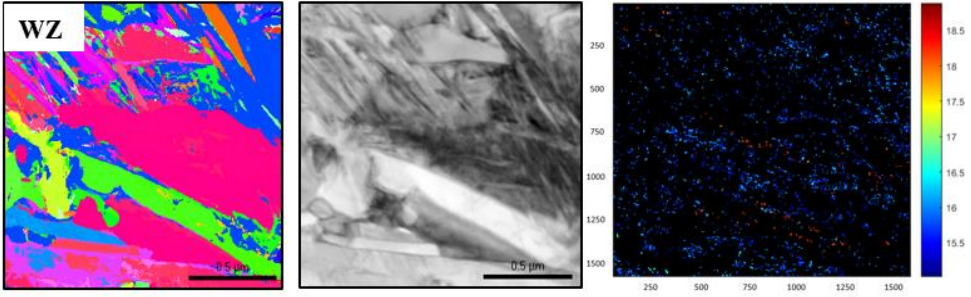
PM
 $10^{17.0814} \text{ m}^{-2}$



TMAZ
 $10^{16.5405} \text{ m}^{-2}$



WZ
 $10^{16.9142} \text{ m}^{-2}$

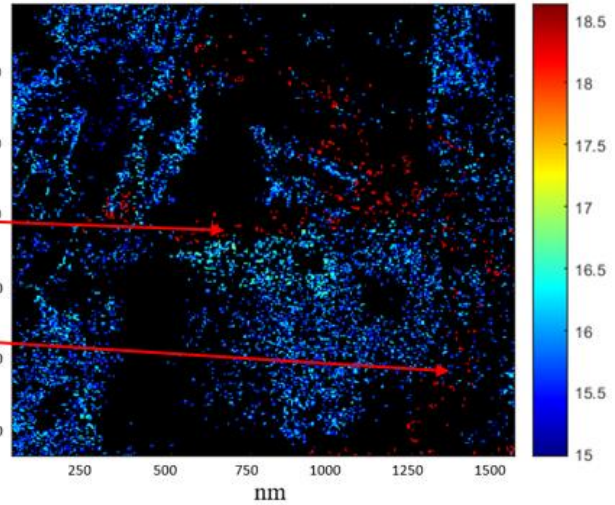
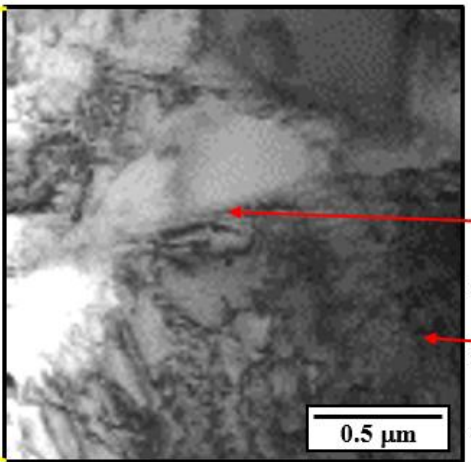
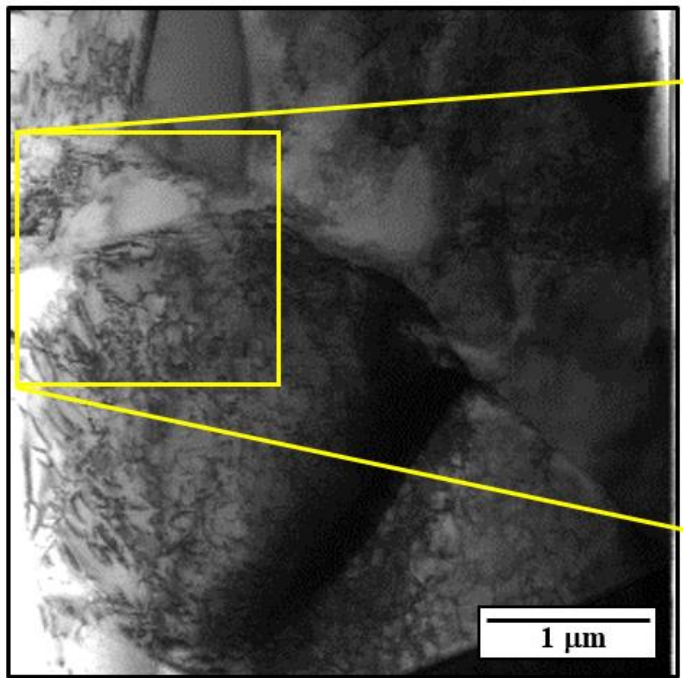


Orientation Virtual Bright Field Dislocation Density Map

Dislocation Density Analysis of LFW Zones



The parent material PM does not have plastic deformation during LFW. Therefore, strain hardening does not occur to increase dislocation density. In contrast, the high presence of bending contours in PM creates the artifact of a higher dislocation presence



Bright field images of PM

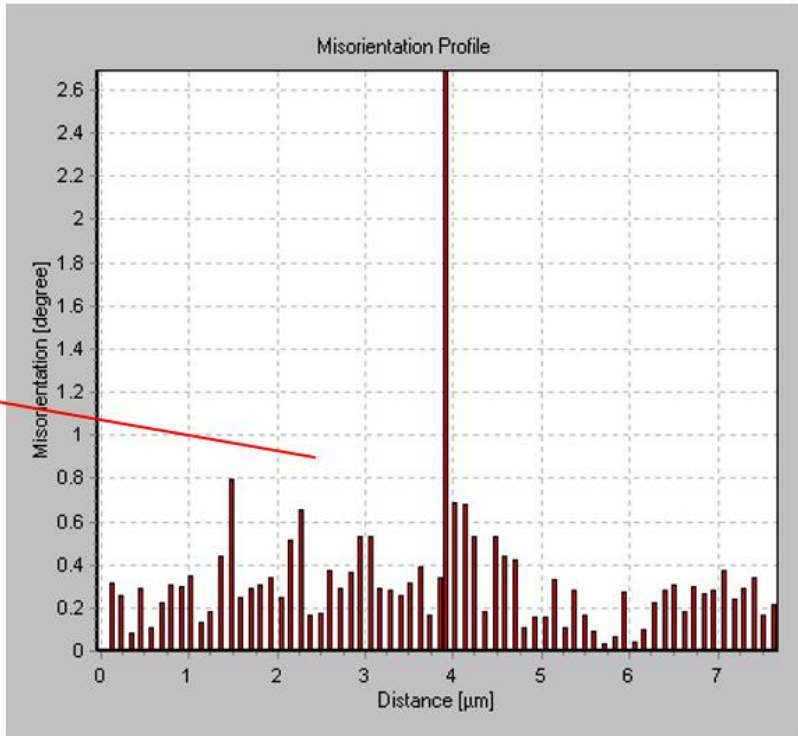
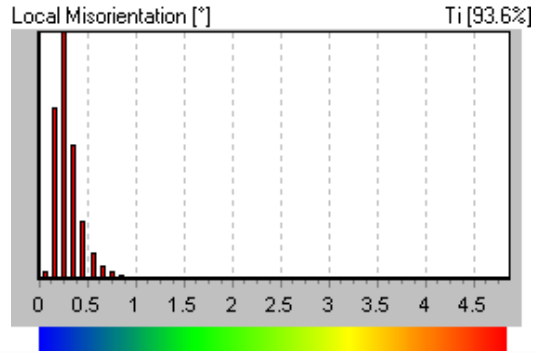
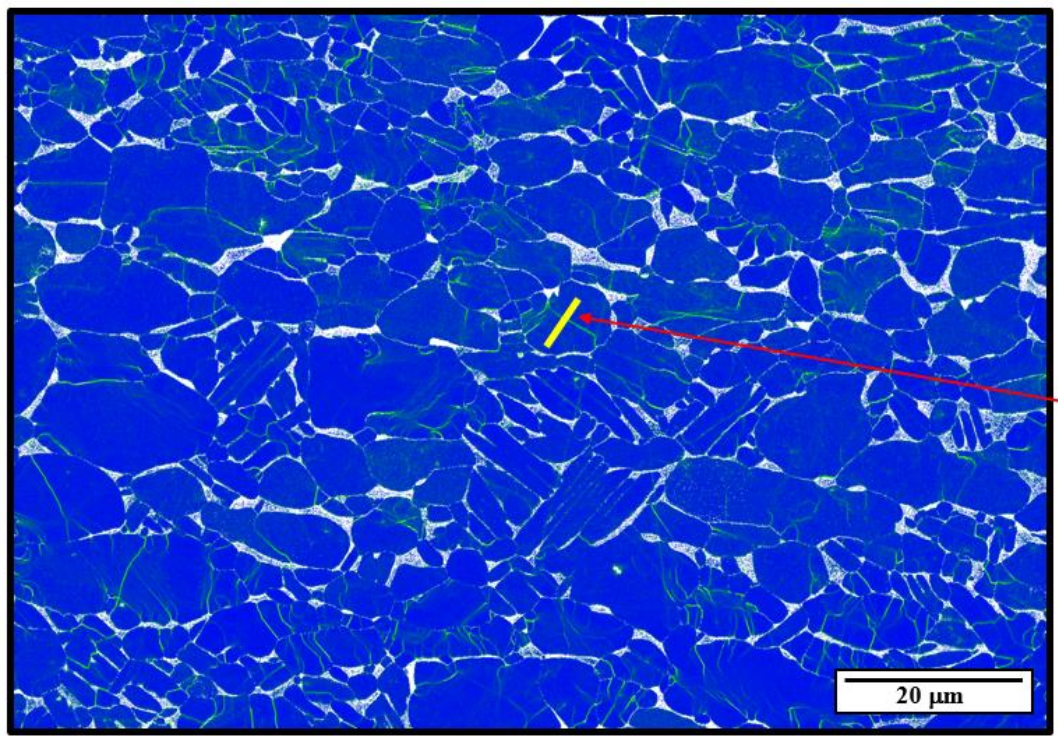
Dislocation density map of PM

Deformation Based on Local Misorientation



Qualitative description of lattice distortion associated to local misorientation

KAM map of PM (1st neighbor, 5° threshold angle)

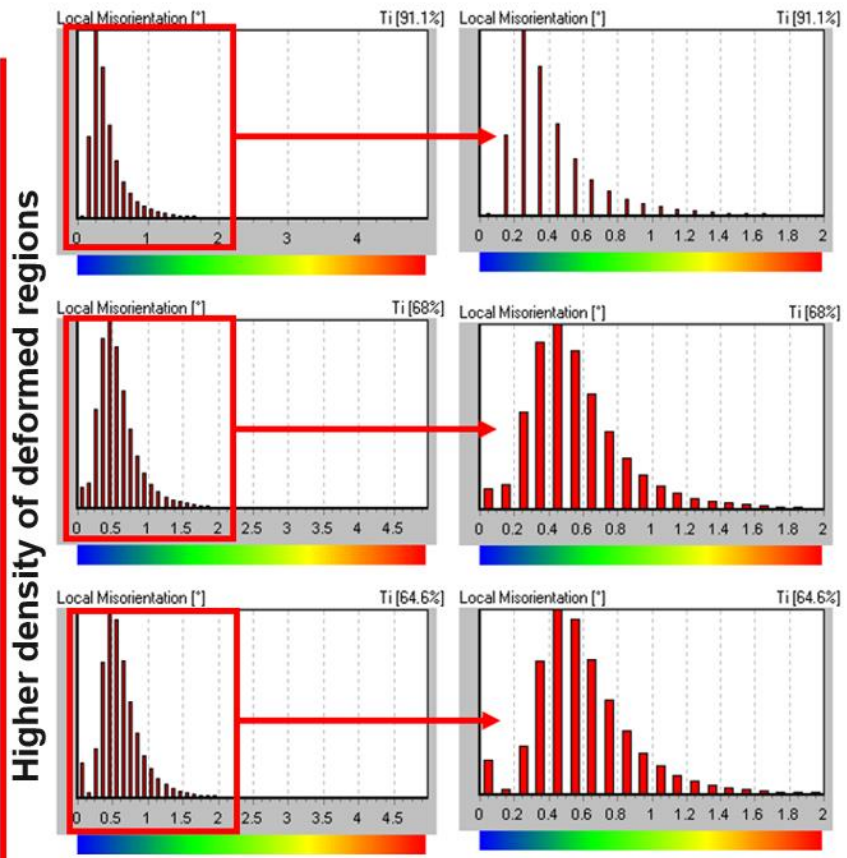
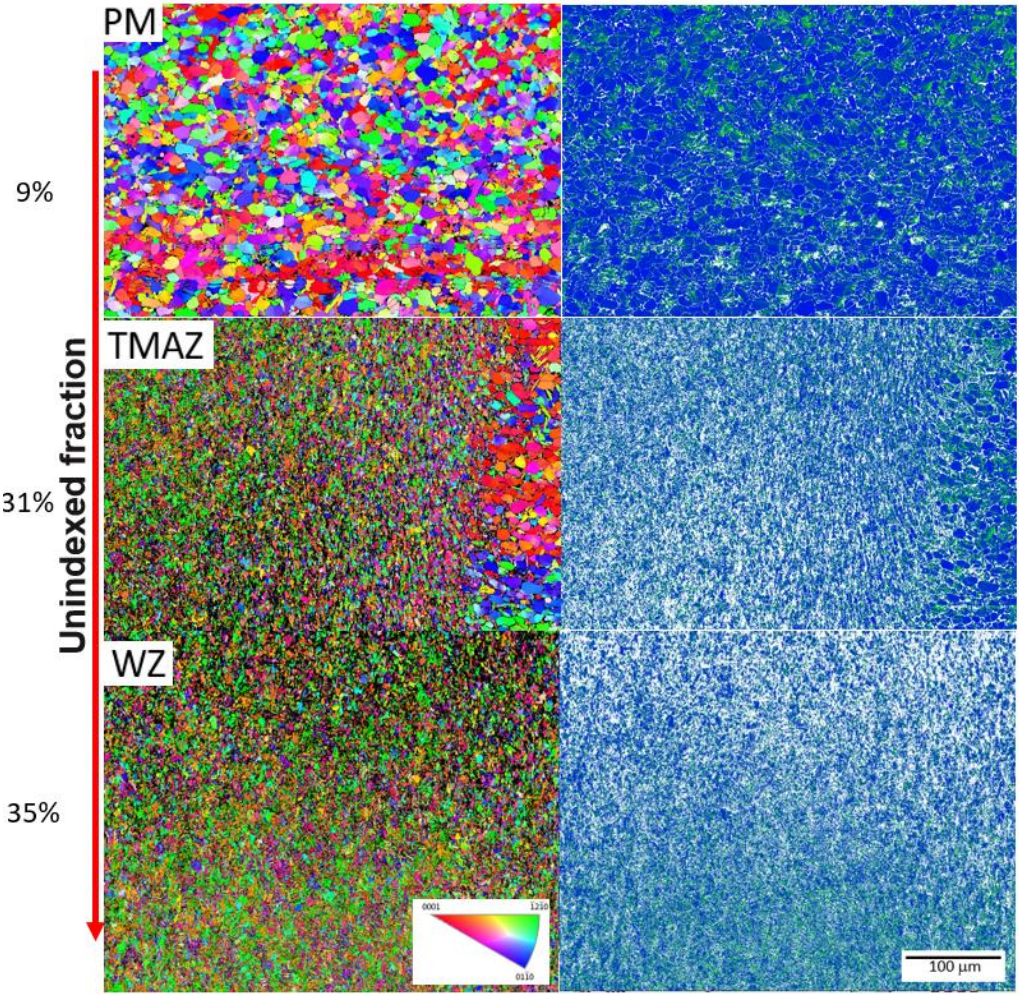


Deformation Based on Local Misorientation



EBSD maps

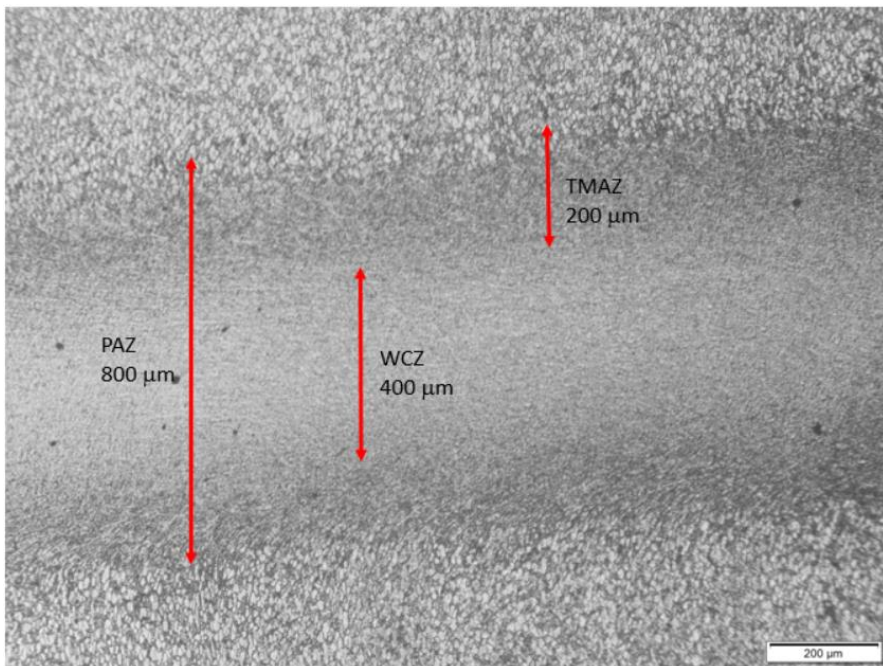
KAM map (1st neighbor, 5° threshold angle)



The kernel average misorientation maps show a trend in density of deformed regions.

Fatigue Approach

Tensile properties are important, but fatigue analysis is also necessary due to the presence of cyclic stresses on Ti-6Al-4V aircraft components.



LFW-Ti-6Al-4V

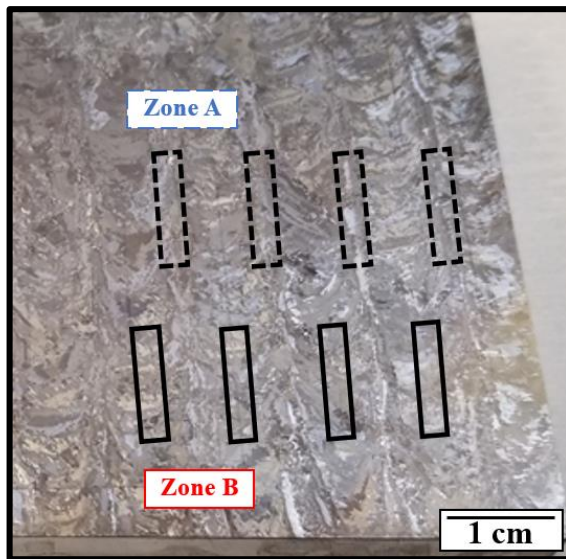


EBAM-Ti-6Al-4V

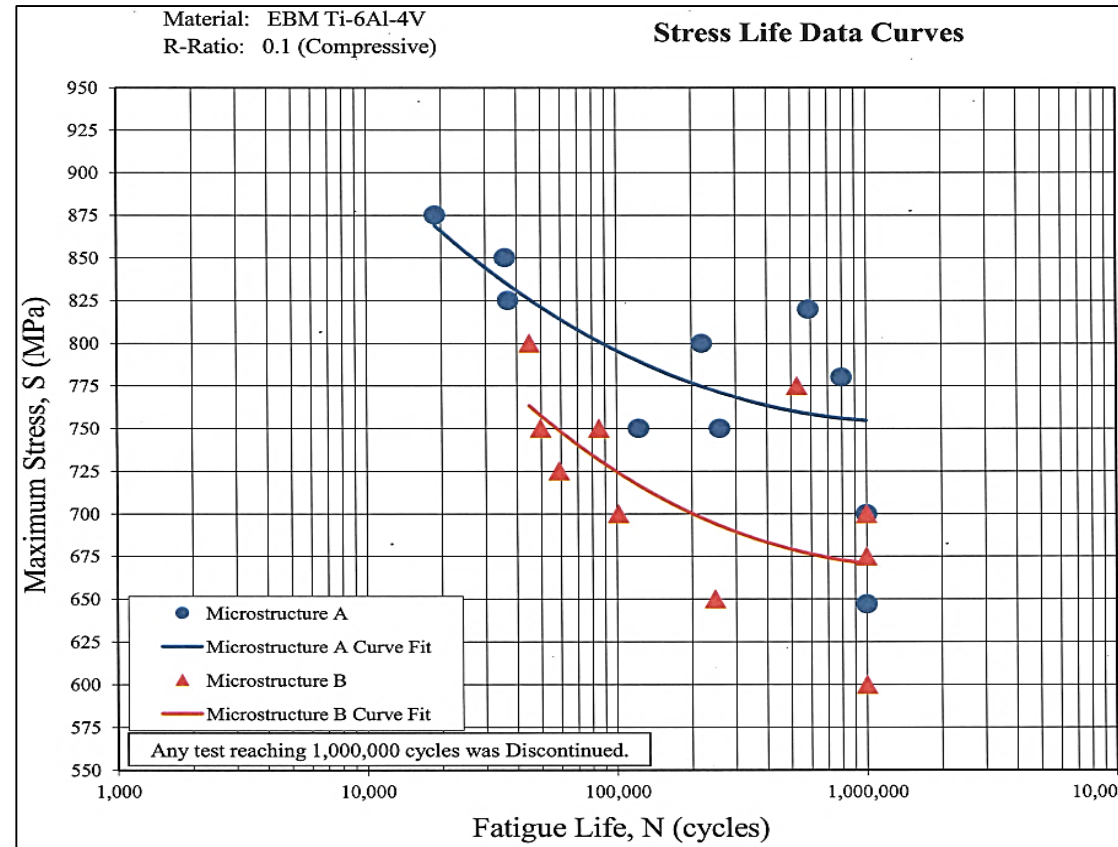
Conventional Fatigue on EBAM-Ti-6Al-4V

Microstructure **A** (blue) has a better fatigue performance than **B** (red) from the S-N curve. The analysis to explain how the microstructure affects that behavior can be divided into two perspectives:

1. Crack initiation perspective
2. Crack propagation perspective



Microstructure **A** and **B** from EBAM-Ti-6Al-4V



Stress life data reported by Westmoreland, Inc.

Crack Initiation Perspective

Cyclic loading of metals undergoes plastic strain localization which leads to the formation of bands or concentrated slip.

The three basic types of crack initiation

- **Initiation at fatigue slip bands**

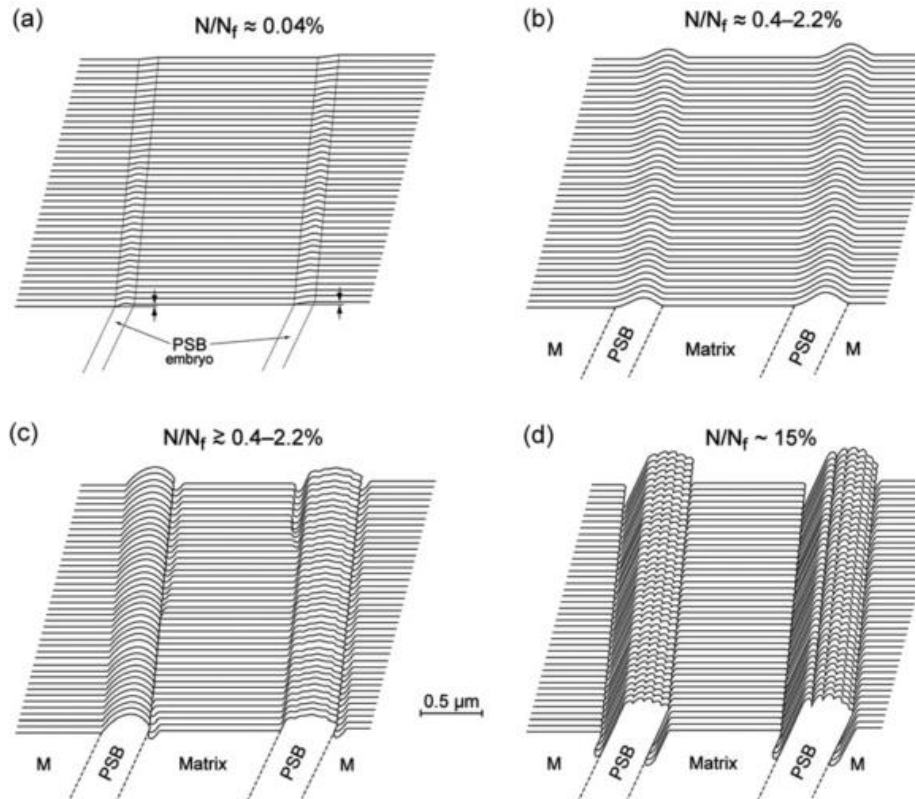
Localization of cyclic slip resulting in development of surface hill-and-valley topography (persistent slip bands PSBs)

- **Initiation at grain and twin boundaries**

The cracks initiate at the large-angle grain boundaries at sites where the PSBs impinge on them

- **Initiation at inclusions, pores and other inhomogeneities**

In some cases the PSBs interact with the inhomogeneities and the cracks initiate at the sites of this interaction



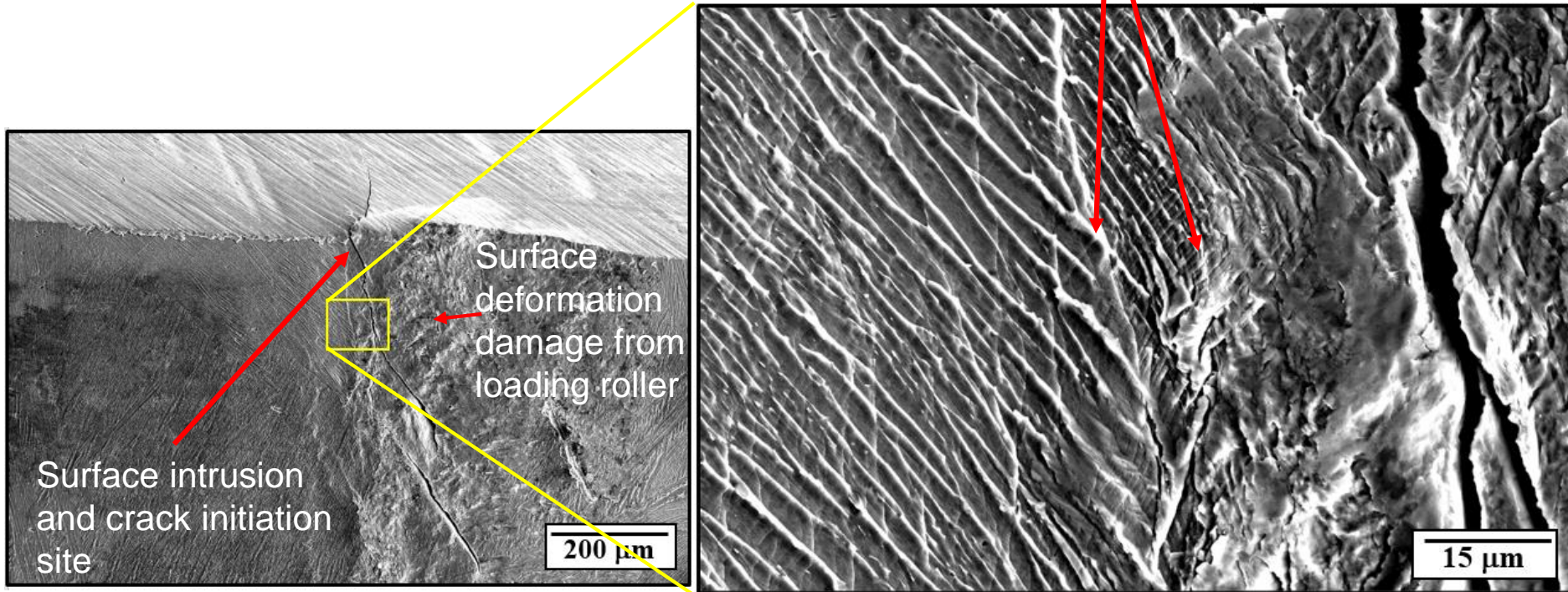
Stages of surface relief evolution to form (b) ribbon-like extrusions and (d) mature PSBs with well developed intrusions at both PSB-matrix interfaces.

• J. Man, P. Klapetek, O. Man, A. Weidnert, K. Obrtlík, J. Polák, Extrusions and intrusions in fatigued metals. Part 2. AFM and EBSD study of the early growth of extrusions and intrusions in 316L steel fatigued at room temperature, Philosophical Magazine 89(16) (2009) 1337-1372 DOI: 10.1080/14786430902917624.

Crack Initiation Site

Specimen **B-2** of 700 Mpa of maximum stress and 101,753 cycles to failure showing an example of a crack initiation site from a developed intrusion.

Different size of slip bands near to the crack



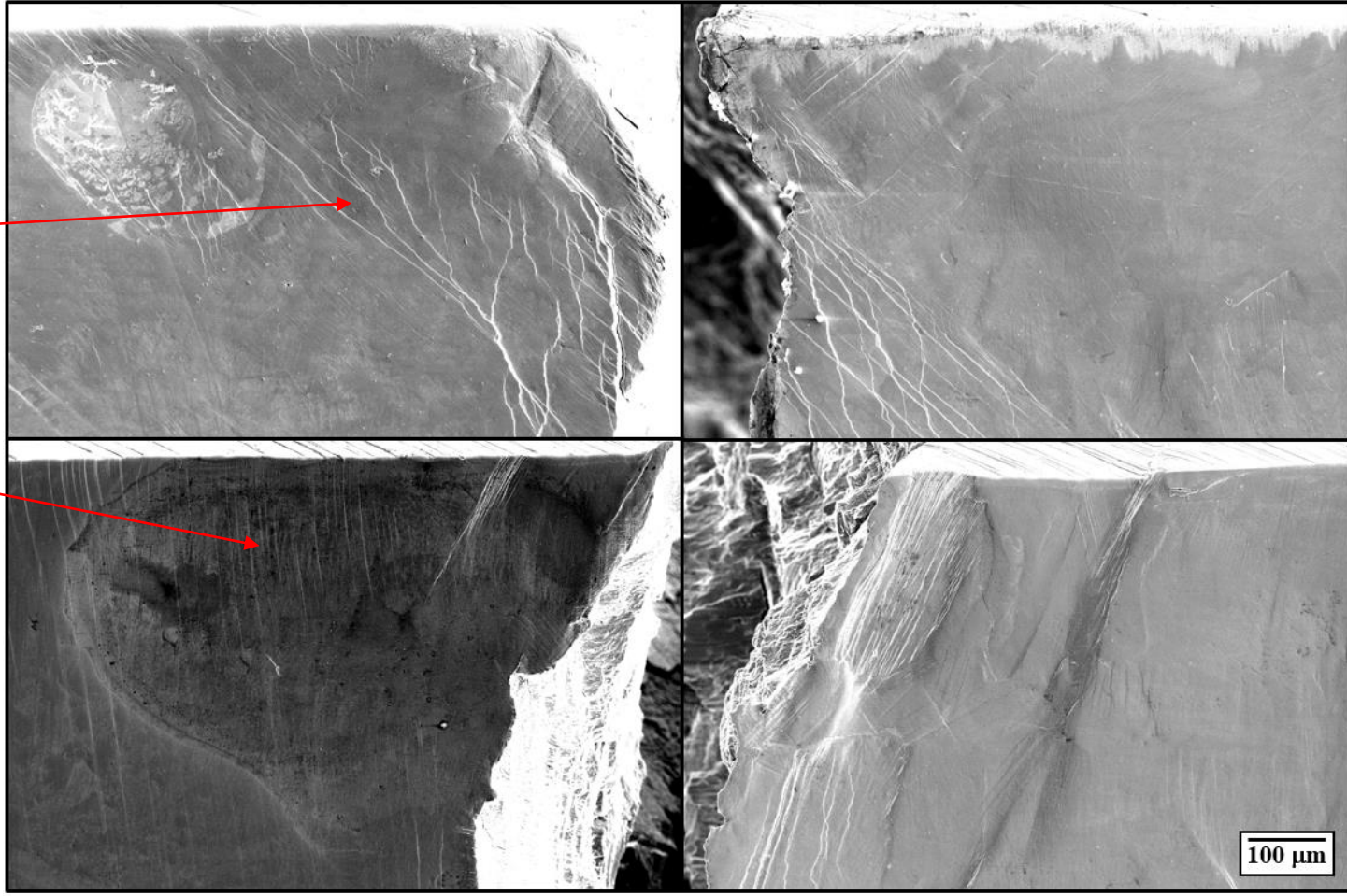
Secondary-electron images of one side of **B-2**

Comparing Microstructure A with B under similar conditions (quantifying slip lines)

B-9
Slip lines total length 5487 μm

Slip lines at B are at a clear higher stage of formation than A

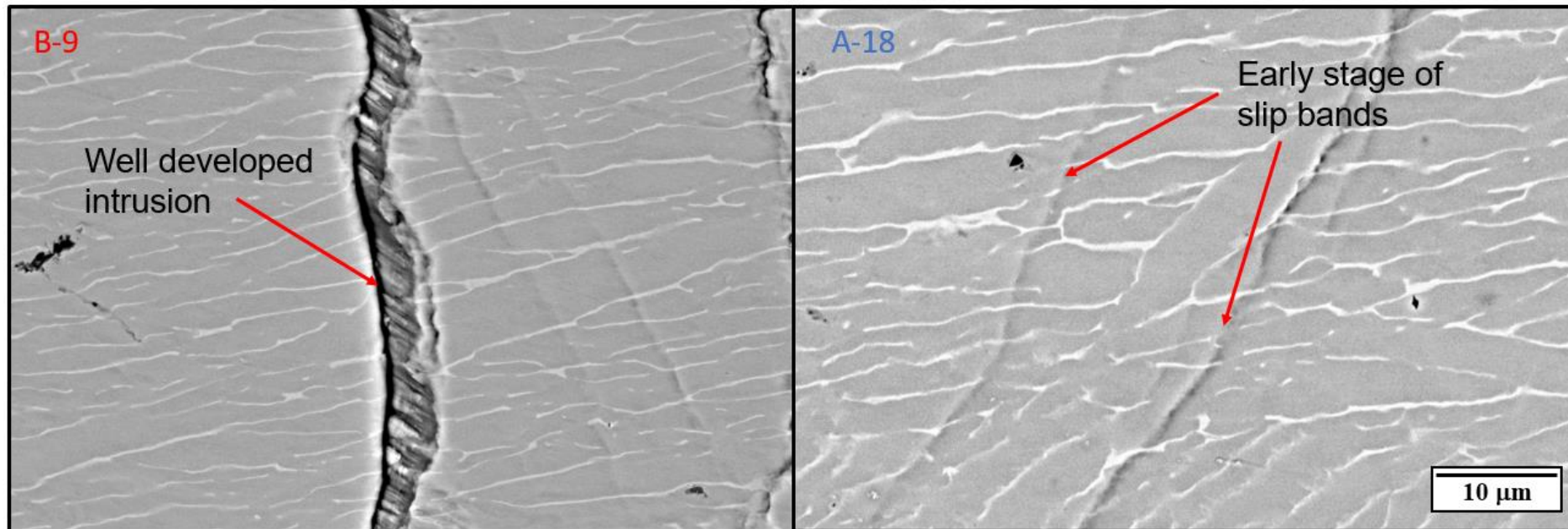
A-18
Slip lines total length 6468 μm



Secondary electron images

Comparing Microstructure A with B under similar conditions

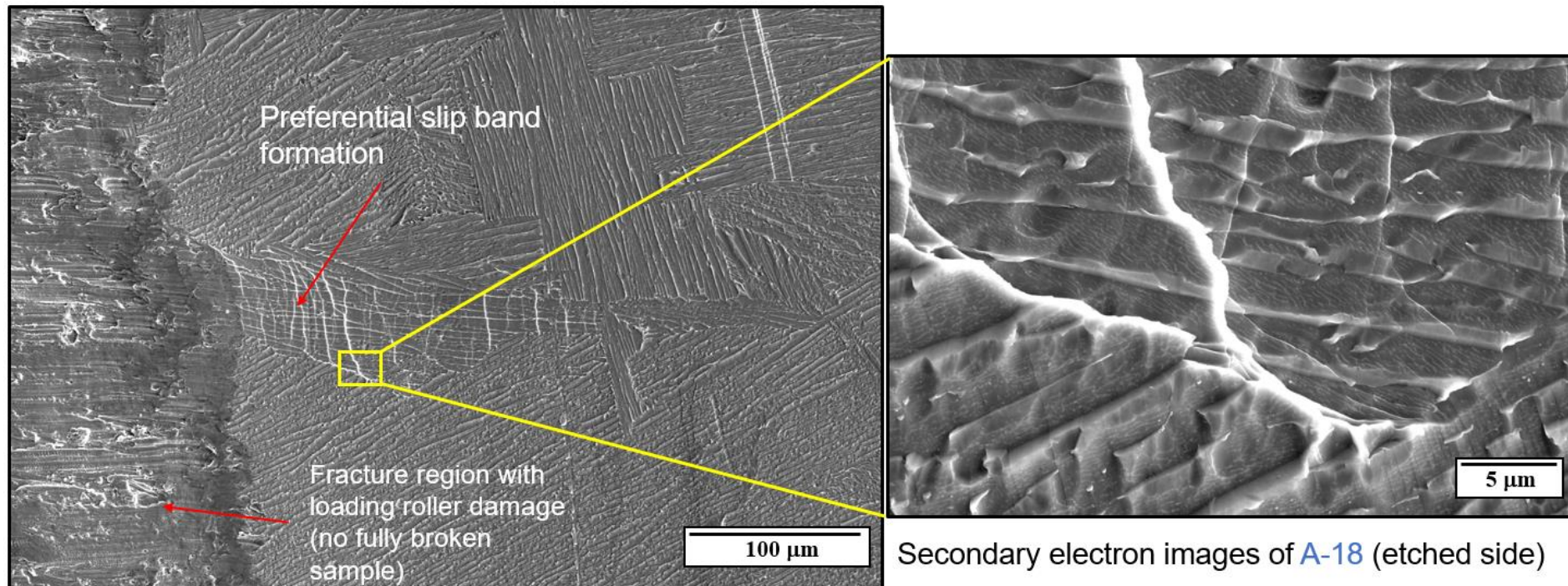
The quantification of total slip lines length on the secondary electron images shows just 15% greater value for **A-18** compared with **B-9**. However, there is a huge difference in the stage of surface relief evolution and a clear development of intrusion on **B-9** compared with **A-18**



Backscatter images of **B-9** (800 MPa and 44,884 cycles) and **A-18** (800 MPa and 220,108 cycles) showing the different stage of slip bands formation

Comparing Microstructure A with B under similar conditions

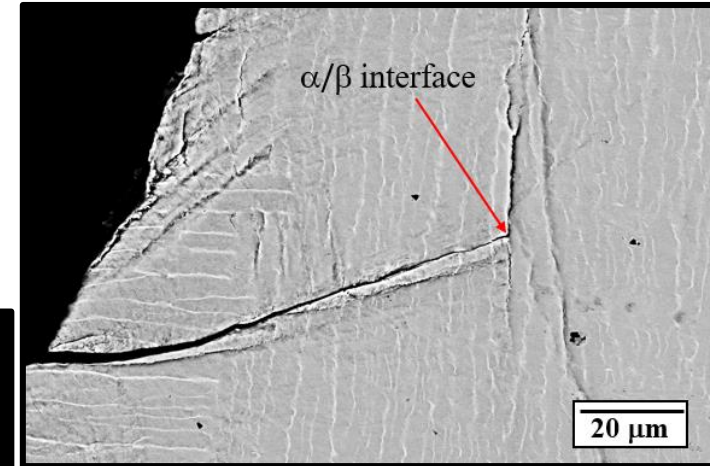
More analysis on microstructure **A** suggests a preferential slip formation depending on a colony orientation respect to the loading direction. Microstructure **B** has a more random a colony orientation offering more opportunity to the best orientation for slip band formation respect to the loading direction.



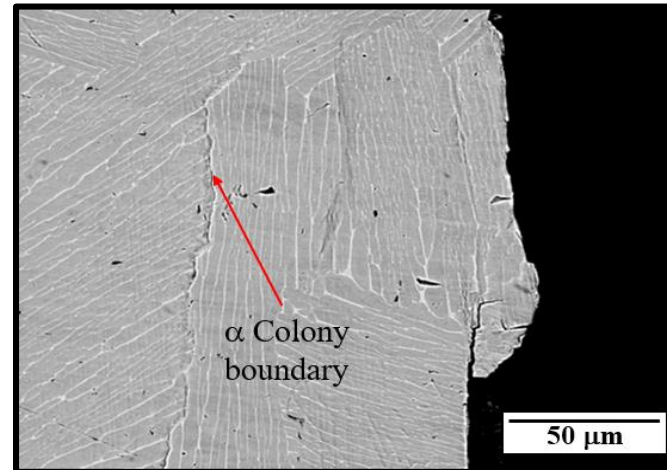
Crack Propagation Perspective

In this fully lamellar microstructure slip or crack propagation barriers are α/β interface < α colony boundaries < Prior- β grain boundaries:

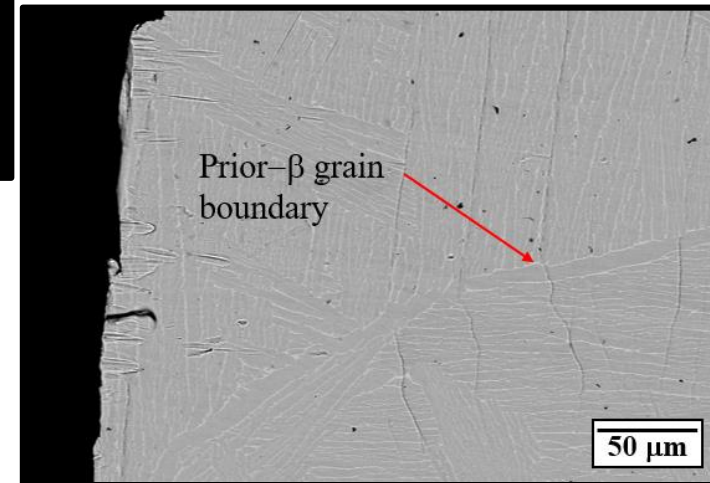
1. α/β interface where slip can be transferred by the parallel slip system $(110) [1\bar{1}1]_{\beta} \parallel (0002)[11\bar{2}0]_{\alpha}$ or others that are off by only 10° .



2. α colony boundaries



3. Prior- β grain boundaries



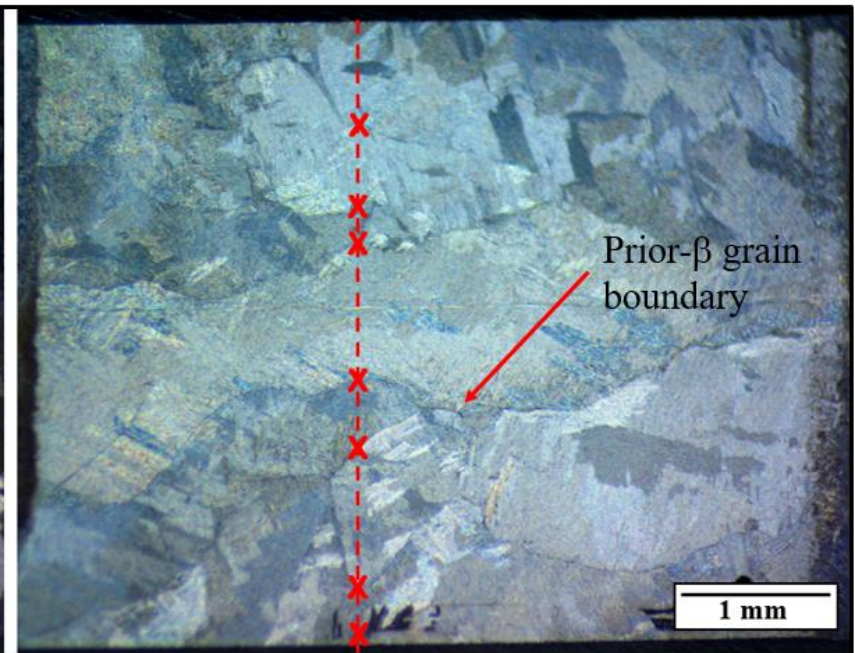
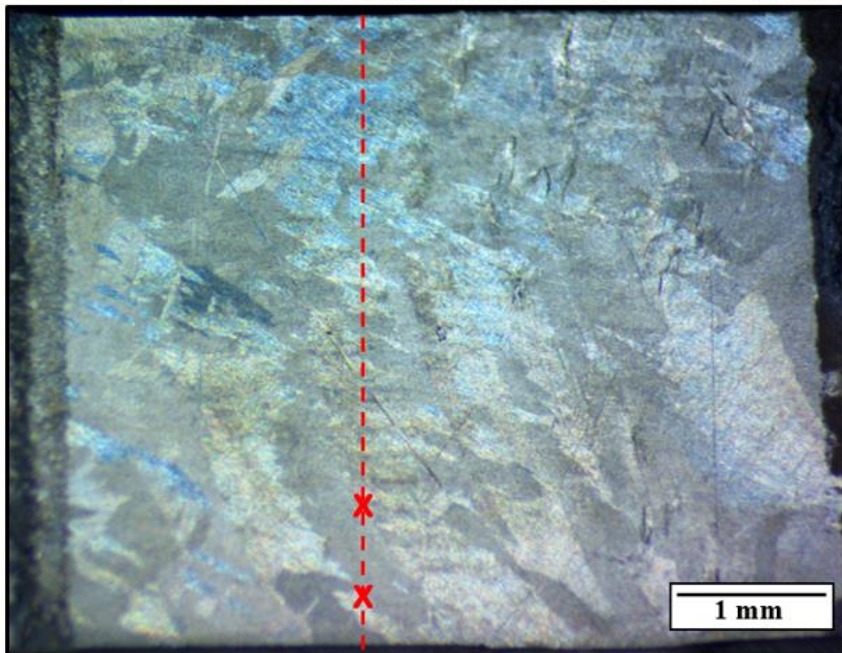
Comparing Microstructure A with B under similar conditions

Prior- β grain boundaries are the stronger barriers and are statistically more present in microstructure of specimen **A-12** compared with specimen **B-2**. Both specimens were tested at a maximum stress of 700 Mpa, but **B-2** failed at 101,753 cycles and **A-12** reached 1,000,000 cycles and was discontinued (Runout).

B-2



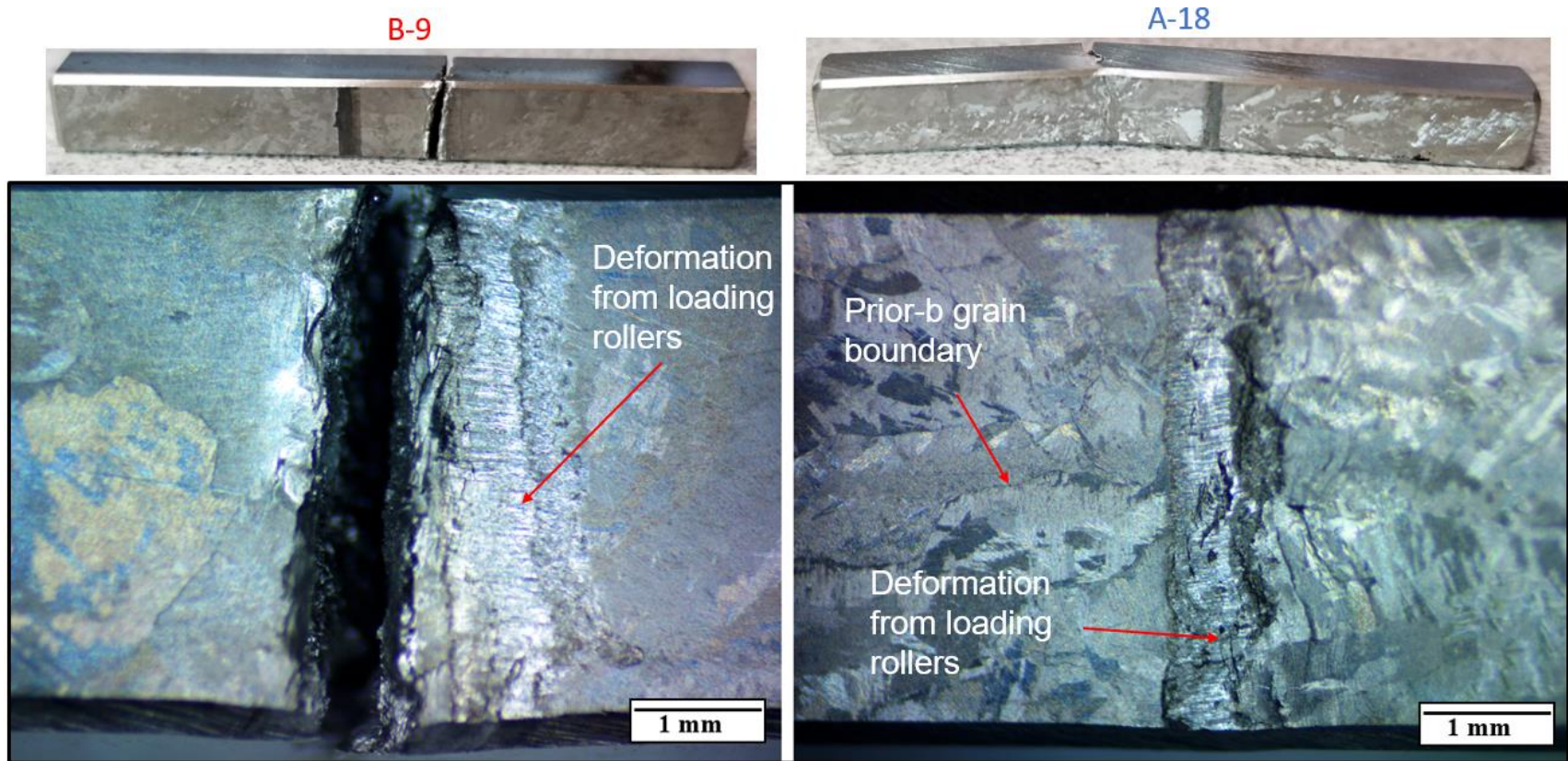
A-12



Optical images of **B-2** and **A-12** specimens

Comparing Microstructure A with B under similar conditions

A-18 has more prior- β grain boundaries and lower degree of deformation than **B-9**. Both specimens were tested at a maximum stress of 800 Mpa, but **B-9** failed at 44,884 cycles and **A-18** failed at 220,108 cycles.



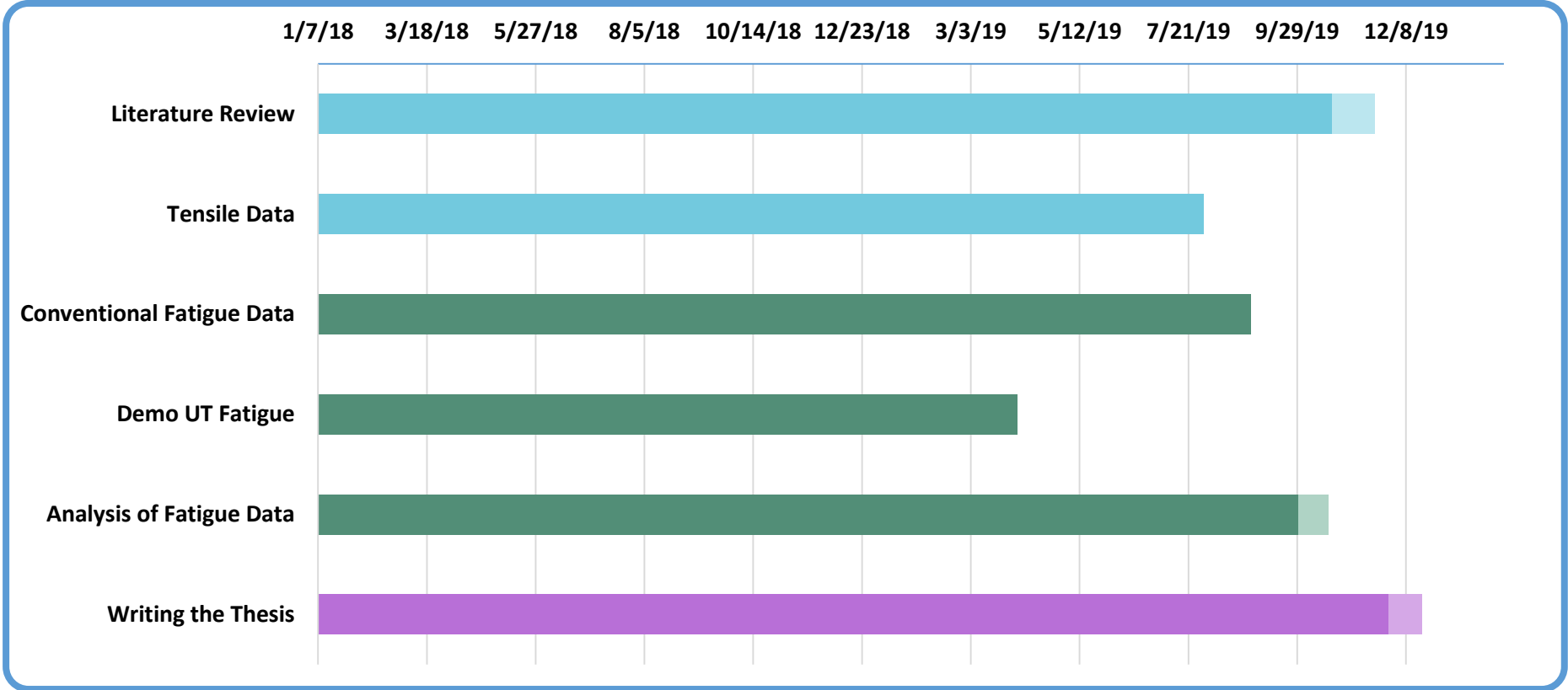
Optical images of **B-2** and **A-12** specimens

Summary of Future Work



- Dislocation density calculation via X-Ray diffraction or alternative method
- S-N curve construction and analysis from ultrasonic fatigue test
- Analysis and comparison of the fatigue tests for validation

Progress Gantt Chart



Challenges and Opportunities



- Dislocation density calculation with a method that provides the good spatial resolution of PED and representative size measurement as in X-Ray diffraction.
- More experimental ultrasonic fatigue test at very high cycle regimes with small specimens for individual microstructure evaluation.

The authors acknowledge the support of the Center for Advanced Non-Ferrous Structural Alloys (CANFSA), an NSF Industry/University Cooperative Research Center (I/UCRC) between Iowa State University and The Colorado School of Mines.

The authors also acknowledge the support of the Defense Advanced Research Projects Agency (DARPA)

Thank you very much!

Michael Mendoza

mym@iastate.edu

Project 35 - On the Influence of Microstructural Features of Linear Friction Welding and Electron Beam Additive Manufacturing Ti-6Al-4V on Tensile and Fatigue Mechanical Properties

Student: *Michael Mendoza*

Faculty: *Peter Collins*

Industrial Partners: *Honeywell*

Project Duration: *January, 2017 – July 2019*

Achievement

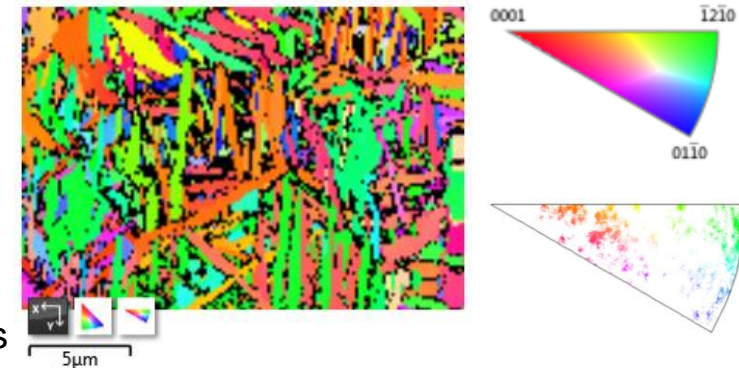
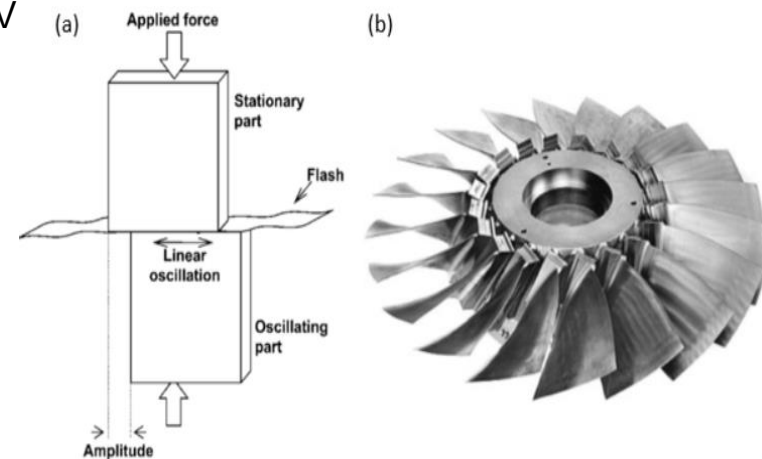
- Characterize local microstructures of Linear Friction Welding (LFW) and their relationship with mechanical properties.

Significance and Impact

- New welding methods as LFW offers cost reduction for aircraft structural components production. Understanding the microstructure-properties relationship in the process is a key factor to its implementation.

Research Details

- Microstructure characterization of individual LFW-Ti-6Al-4V zones to evaluate tensile properties and exploration of fatigue analysis on larger local microstructures as EBAM-Ti-6Al-4V for future applicability on LFW.



Project 35 - Characterization of Microstructures and Mechanical Properties in LFW Ti-6Al-4V



CANFSA
CENTER FOR ADVANCED
NON-FERROUS STRUCTURAL ALLOYS

Student: *Michael Mendoza*

Faculty: Peter Collins

Industrial Partners: *Honeywell*

Project Duration: *January 2017 – July 2019*

Achievement

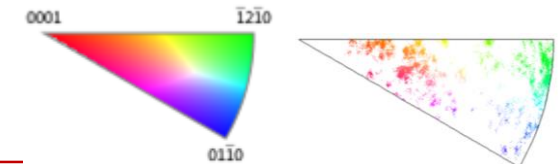
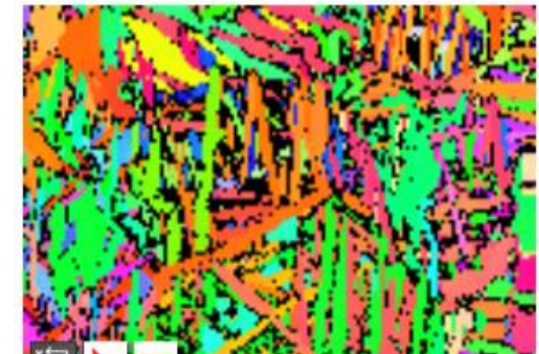
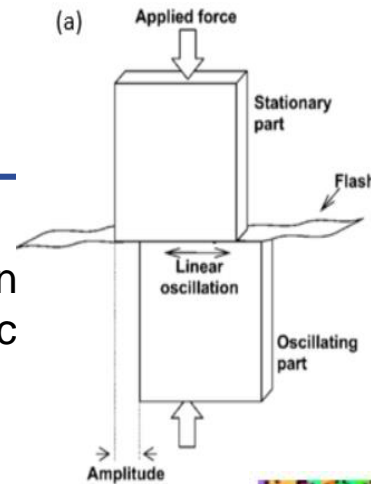
- Characterize local microstructures of Linear Friction Welding (LFW) and their relationship with mechanic properties

Significance and Impact

- New welding methods as LFW offers cost reduction for aircraft structural components production. Understanding the microstructure-properties relationship in the process is a key factor to its implementation.

Research Details

- Microstructure characterization of individual LFW-Ti-6Al-4V zones to evaluate tensile properties and exploration of fatigue analysis on larger local microstructures as EBAM-Ti-6Al-4V for future applicability on LFW.



Project 35 - Characterization of Microstructures and Mechanical Properties in LFW Ti-6Al-4V

Student: *Michael Mendoza*

Faculty: *Peter Collins*

Industrial Partners: *Honeywell*

Project Duration: *January. 2017 – July 2019*

Program Goal

- Characterize the microstructure and mechanical properties of Linear Friction Welding (LFW)

Approach

- Evaluate tensile properties on LFW-Ti-6Al-4V and explore fatigue analysis on larger microstructures as EBAM-Ti-6Al-4V for future applicability on LFW.

Benefits

- The understanding of microstructure-properties relationship of LFW will improve manufacturing efficiency of aircraft components.

